Laser-Wakefield Application to Oncology

B. S. Nicks*, T. Tajima and D. Roa
University of California, Irvine, CA 92697, USA
**bnicks@uci.edu*

A. Nečas
TAE Technologies, Inc., Foothill Ranch, CA 92610, USA

G. Mourou
École Polytechnique, Palaiseau, 91128, France

Recent developments in fiber lasers and nanomaterials have allowed the possibility of using laser wakefield acceleration (LWFA) as the source of low-energy electron radiation for endoscopic and intraoperative brachytherapy, a technique in which sources of radiation for cancer treatment are brought directly to the affected tissues, avoiding collateral damage to intervening tissues. To this end, the electron dynamics of LWFA is examined in the high-density regime. In the near-critical density regime, electrons are accelerated by the ponderomotive force followed by an electron sheath formation, resulting in a flow of bulk electrons. These low-energy electrons penetrate tissue to depths typically less than 1 mm. First a typical resonant laser pulse is used, followed by lower-intensity, longer-pulse schemes, which are more amenable to a fiber-laser application.

Keywords: Brachytherapy; fiber lasers; laser wakefield; electron beams; critical density; sheath physics.

1. Introduction

The treatment of cancer remains one of the most pressing concerns of medical research. One promising avenue of cancer treatment is brachytherapy, in which a source of radiation is brought inside the body close to the tissues requiring treatment.[1] This technique localizes the radiation dose to source of radiation, limiting collateral damage to surrounding healthy tissue. In contrast, more conventional external sources of radiation can cause significant damage to intervening tissues. Typically, small quantities of radioisotopes provide the dose source for brachytherapy, but such sources suffer from decay, which lengthens treatment times, and shielding costs. The use instead of an electron beam as the radiation source would eliminate the first challenge and greatly mitigate the second.

A potential means for generating such an electron beam is Laser Wakefield Acceleration (LWFA),[2] a compact method of accelerating electrons to high energies which was first proposed by Tajima and Dawson[3] in 1979. While conventional linear accelerators (LINAC), relying on large and costly wave-guide cavities, are limited in acceleration gradient by the breakdown threshold of metals, the strong

electric fields accessible in plasmas (which are already broken-down) allow much higher accelerating gradients: GeV per cm or higher. Such a high acceleration gradient reduces the necessary machine size and also increases their availability through reduction in cost. Typical electron energies needed for brachytherapy lie in the range between 100 keV and 5 MeV, and thus LWFA can accelerate electrons to these energies in micron to millimeter scale lengths. LWFA was demonstrated experimentally[4,5] after the invention of Chirped Pulse Amplification (CPA),[6] which allowed access to the necessary high intensity laser regime. Since then, many more experiments have demonstrated this technique in different regimes, and the field has been growing steadily.

Research in the use of LWFA to generate electron beams for medical applications has proceeded for at least two decades now. Initially, these efforts focused on generation of high-quality electron beams with energies roughly in the range 6–25 MeV, as would be applicable for conventional, external sources of radiation for cancer therapy.[7–13] Recent innovations in the field of fiber lasers has offered a new leap forward in this effort: the Coherent Amplification Network (CAN),[14] in which many individual micron-scale fiber lasers are coherently combined and amplified to provide both high-rep rate and high power. This innovation allows medical LWFA to proceed into a new regime of applications, though a CAN laser certainly is applicable as well to the traditional medical effort at producing an external electron beam.

As we see below, we find that even at very modest intensity, LWFA can produce electrons that are relevant for tissue penetration and delivery of beams of ionizing radiation. With this insight, in combination with the compactness afforded by the recent developments in fiber lasers, we are led to consider the new situation of *in situ* radiation sources (of electrons). In this vision, we see three chief schemes in which the wakefield electron source could be brought directly to the cancer. First, the laser-wakefield accelerator could be inserted in an intraoperative fashion,[10,11] which involves surgically opening the intervening tissues and can presently be used for LINAC sources in some instances. A surgeon may also use such an operation to remove any residual cancer or clean affected tissues by hand. Less invasive is brachytherapy, where the laser is injected discreetly into the body, such as through a blood vessel or directly through tissue. Finally, it may be possible to carry the laser into the body in a endoscope, whereby the surgeon could potentially both diagnose and treat the cancer simultaneously. It is our goal here to devise a way in which any or all of these methods might be possible with LWFA.

In each of these cases, the electrons beam need only have shallow penetrative power, as they need not traverse the body before reaching the tissues to be treated. The desirable energy for an electron beam then reduces to the order of 10^2 keV. We thus seek a means of producing low-energy electrons. The electron energy gain from LWFA is given by $\Delta\mathcal{E} = 2g(a_0)m_ec^2(n_c/n_e)$, where a_0 is the normalized laser intensity, $g(a_0)$ represents the function dependence of energy gain on a_0, n_c is the

laser critical density, and n_e is the plasma density.[3] This relation suggests a path to low-energy electrons through a high plasma density and modest laser intensity, parameters that are also favorable to fiber lasers, as will be discussed. To provide a target material near the critical density of an optical laser ($n_c = 1.11 \times 10^{21}$ cm^{-3} for a laser wavelength of 1 micron), it may be best to use a porous nanomaterial,[15–17] such as porous alumina or carbon nanotubes, as is the main focus of this workshop. Such a target material for irradiation by the laser would also avoid the presence of ionized gas inside the body.

While the low-density, high-energy regime of LWFA has been studied extensively, the high-density, low-energy regime has been less explored in detail.[18] Indeed, the expression for electron energy gain given above was established by studying the low-density regime. As a foundation for these applications, the physics of the high-density regime of LWFA has been recently studied in Nicks *et al.*, 2019.[19] This work studied first the scaling laws of the electron energy gain for n_c/n_e and a_0. It was found that $g(a_0)$ is well-represented by the ponderomotive potential $g(a_0) = \sqrt{1 + a_0^2} - 1$. Additionally, it was found that $\Delta\mathcal{E} \propto n_c/n_e$, the proportionality predicted by low-density wakefield theory, was obeyed in the regime $n_c/n_e \gtrsim 1$ for the highest-energy electrons. Next, the mechanics of electron acceleration in the regime $n_c/n_e \sim 1$ were studied, revealing sheath acceleration[20] that generates a peculiar stream-like distribution of bulk electrons in phase space. This bulk acceleration by sheath contrasted significantly with the trapping and acceleration seen in low-density wakefield. This work then attempted to quantitatively distinguish this high-density, sheath regime from the more typical wakefield physics seen at low densities. Finally, this work briefly examined the penetrative power of such an accelerated spectrum of electrons in water, approximating biological tissue.

2. Acceleration in the High-Density Regime

To study laser-wakefield physics in the high-density regime, we use the 1D particle-in-cell (PIC) code EPOCH. An optical ($\lambda = 1$ micron) laser is injected from vacuum into a uniform slab of plasma with a temperature of 100 eV. First, we seek to understand the wakefield physics at high density with an approach that may be impractical with regard to fiber lasers but more easily understood in the context of typical wakefield physics. We first use a flat-top resonant laser pulse, which has a pulse length equal to half of the wakefield wavelength, and the plasma density is taken to be the laser critical density. The laser intensity is taken to be the somewhat powerful value of $a_0 = 1$. A resonant laser pulse in a plasma near the critical density ($n_c/n_e \leq 2$) must necessarily be sub-cycle, or at most single cycle. While sub-cycle lasers have been demonstrated experimentally,[21,22] such a setup would be generally difficult to implement, particular in a fiber laser.[14] Instead, a long, self-modulating pulse would be much more practical a fiber laser application, as is discussed in Sec. 3. It will be shown that with a longer pulse the essential physics remains unchanged.

The interaction of the laser with the plasma in the two contrasting regimes of high and low density has a convenient analogy in tsunami waves in a certain property of the wave dynamics. The phase velocity of the wake field matches the laser group velocity in the plasma ($v_g = c\sqrt{1 - n_e/n_c}$), much as sea-floor depth determines the phase velocity of an ocean wave. In the open ocean, where the water depth is great, tsunami waves propagate with a fast phase velocity and thus do not couple to stationary objects. Boats in the ocean, for instance, may move slightly in the transverse direction (vertically), but are not otherwise affected. The waves in this regime also do not couple to the sediment on the sea floor, and so remain "blue". An object such as a surfer could only be trapped and accelerated by these waves by exerting a great deal of effort to approach the wave phase velocity. So it is with wakefield: in the low-density regime, the wake phase velocity is near the speed of light, and while a small number of elections may be accelerated to high energies, the wake does not couple to the bulk motion of the plasma. The wake and accelerated electrons form a clean and coherent train.

Near the shore, however, the increasingly shallow water causes the phase velocity of the wave to slow down, which leads to amplification and steepening of the wave until breaking occurs. The slow velocity of the wave near the shore then causes catastrophic "trapping" of stationary objects. Additionally the slow wave velocity couples with turbulence created by wave breaking to create anomalous transport on the sediment bed. Significant amounts of sediment quickly pass into the wave, creating a visibly "black" tsunami from the clean, "blue", off-shore starting wave and leading to momentum transport of the sediment.[19,23] Similar physics occurs in wakefields near the critical density. The laser couples strongly to the bulk motion of the plasma, creating a qualitatively distinct regime that features sheath acceleration and bulk flow of electrons.

The typical approach to LWFA, which seeks to generate high-energy electrons, is to use a low-density plasma ($n_c/n_e \gg 1$). In this regime, which we may call the "blue wave" case ($v_g \approx c$), a train of coherent wake waves follows the laser pulse. This wake then accelerates a regular train of electrons. The wakefield, which is a longitudinal electric field, reaches a saturation value on the order of the Tajima-Dawson field[3,24]: $E_{TD} = m_e\omega_p c/e$, where ω_p is the plasma frequency. This state of affairs reigns until the laser has traveled either the dephasing length, at which electrons begin to decelerate, or the pump depletion length, at which the laser has lost significant energy to the plasma and can no longer excite a robust wakefield. The high group velocity of the laser leaves the bulk plasma intact and creates a "blue" wakefield.

In contrast, the case of $n_e = n_c$, the "black wave", shown in Fig. 1, exhibits quite different behavior. Here, $v_g = 0$, restricting the laser-plasma interaction to within one plasma wavelength. The long train of trapped electrons in the low-density case becomes replaced by streams of low-energy ($\Delta\mathcal{E} \sim 100$ keV) electrons ejected from the site of laser entry roughly every plasma period. These electrons are accelerated

by an oscillating sheath that is formed by the laser at the initial boundary of the domain. This behavior is somewhat reminiscent of laser interaction with a solid target and previous sheath acceleration efforts.[20] However, some diminished part of the laser is still able to propagate through the target, and the ions have essentially no response. The "blackness" of the wave derives from its strong coupling to the bulk electrons, which occurs because $v_g = 0$ for the laser, much as an ocean wave that slows down near the shore becomes turbulent and dredges sediment from the sea-floor. As n_e is decreased from the critical density, a transition between the "black" and "blue" regimes is seen, as is shown in Fig. 2 for the "grey" case of $n_c/n_e = 1.7$, which shows elements of the bulk flow of high-density wakefield as well as elements of more typical, low-density wakefield. These sheath mechanics may also be useful for the understanding of related ion acceleration. dynamics[2,25]

The maximum electron energy in the phase-space distribution shown in Fig. 1 is roughly 1 MeV, which is encouraging for the medical aims in this study. A naïve next step to increase the electron dose and alleviate the difficulty with a sub-cycle pulse might then be to increase the length of the laser pulse to produce a larger dose of electrons. Such a case is shown in Fig. 3 for $n_c/n_e = 1$ and a laser pulse length of $\lambda_{lp}/\lambda_p = 8$ for a snapshot at time $t/\tau_p = 96$, where $\tau_p = 2\pi/\omega_p$ is the plasma period. At this time the laser interaction has finished, as well as most of the electron acceleration, and thus this snapshot represents the near-final behavior. The overall interaction with the plasma is much more violent. For $x/\lambda_p \gtrsim 32$ a large body of overlapping electron streams is seen, which originate in the initial laser interaction. For $x/\lambda_p \approx 2$ a longitudinal oscillation similar to that in the resonant pulse case is formed which generates subsequent electron streams. This scheme is also more energetically efficient than that of Fig. 1, indicating that both the quantity and quality of low-energy electron production is improved. However, this case relies on the relatively strong intensity of $a_0 = 1$, which is likely untenable for fiber lasers.

3. High-Density LWFA in Fiber Lasers

Fiber lasers, particularly in coherent networks, offer the potential for high-power and high-rep rate lasers. Yet, individual fibers are also subject to a number of constraints not shared by large, conventional lasers. Perhaps most importantly, the material properties of fibers, which are typically made from silica, place a much more stringent limit on the intensity of the transmitted laser pulse.[26] Certainly for any fiber application inside the body, it is paramount that material damage to the fibers be avoided, as this damage would then harm the surrounding tissue as well, with potentially severe consequences. In addition to the requirement of avoiding ionization of the fiber, an even more restrictive condition may be the level of tolerable accumulation of nonlinear phase in the laser pulse, the severity of which grows with laser intensity. Given this background from the field of fiber optics, a acceptable order of magnitude for laser intensity that safely avoids these issues may be

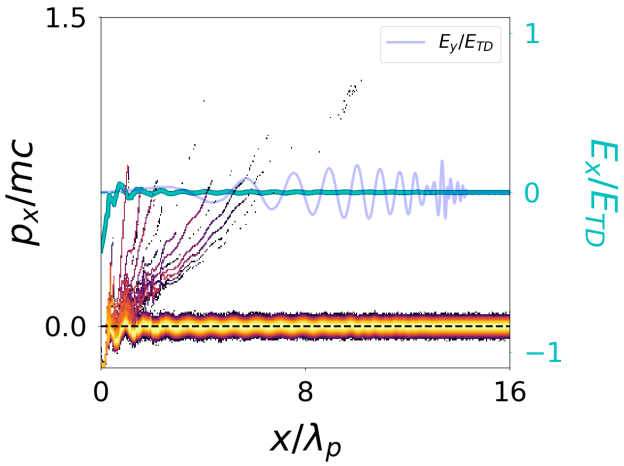

Fig. 1. A snapshot of the electron phase space p_x vs. x (heat-map, with warmer colors representing higher density) and longitudinal E_x (green) and laser E_y (translucent blue) fields for high-density ("black") case $n_c/n_e = 1$ with laser intensity $a_0 = 1$. The plasma wavelength is given by $\lambda_p = 2\pi c/\omega_p$. The time step is $t = 14.4\tau_p$, where τ_p is the plasma period. (Similar run in Nicks *et al.*, 2019.[19])

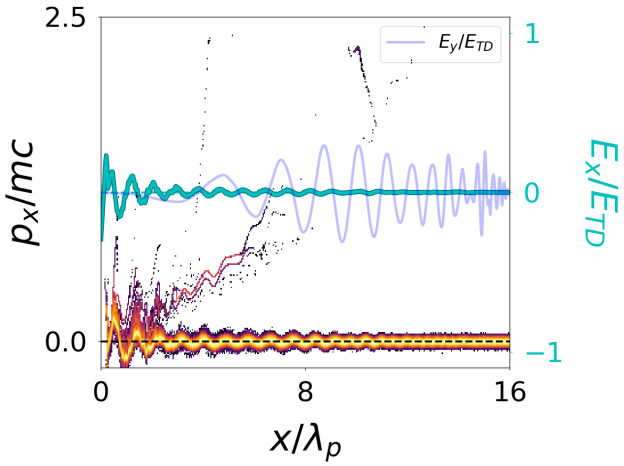

Fig. 2. The electron phase space and field structure of the intermediate ("grey") case of density $n_c/n_e = 1.7$ at the laser intensity $a_0 = 1$. The time step is $t = 16.0\tau_p$

10^{14} W cm^{-2}. We take this value as a starting point, but subsequent technical and material efforts may require a more conservative value. This intensity corresponds

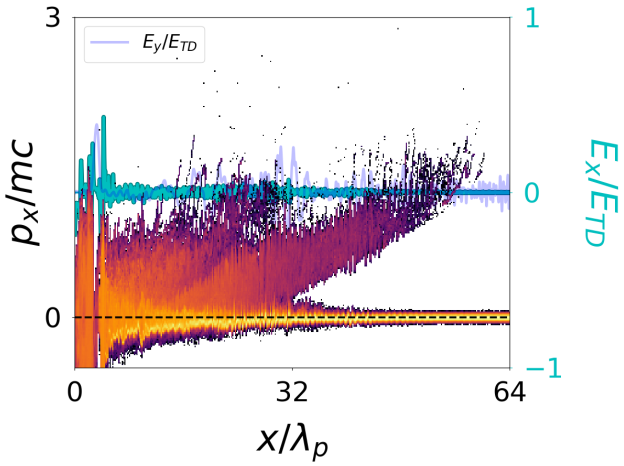

Fig. 3. The electron phase space and field structure of the critical density case $n_c/n_e = 1$ for a laser pulse of length $8\lambda_p$ at the laser intensity $a_0 = 1$, showing the "black tsunami" regime. At this snapshot ($t = 80.6\tau_p$) most of the electron acceleration is concluded and most of the laser has exited the domain. (Similar run in Nicks *et al.*, 2019.[19])

to $a_0 \approx 0.01$, which is far below the relatively powerful value of $a_0 = 1$ considered thus far. The expression for electron energy gain $\Delta\mathcal{E} = 2g(a_0)m_e c^2(n_c/n_e)$, where $g(a_0) = a_0^2/2$ for $a_0 \ll 1$ if $g(a_0)$ takes the form of the ponderomotive potential, suggests that one means of compensating for this low individual fiber laser intensity to attain 10^2 keV electrons is simply to use a coherent network of ~ 100 lasers, though in a endoscopic application this number may be difficult to achieve. Phase-matching each fiber would also be technically difficult, but may be possible making use of the partial reflection of the laser pulse at the boundary between the fiber and high-density material to be irradiated. However, by lowering the target material density, one can use fewer coherent lasers, such as with ~ 10 lasers at $n_c/n_e = 10$. Another alternative is the use of a hollow fiber, which can have a diameter of order 10^2 times larger than that of a typical fiber, thereby accommodating much more pulse energy.

Another chief concern with fiber lasers is the pulse length. While thus far the simulations in this work at $n_c/n_e \approx 1$ have used resonant laser pulse lengths of ~ 2 fs (a difficult, sub-cycle pulse in its own right), the shortest pulse practically achievable for a fiber laser is likely around 100 fs. Letting λ_l be the laser pulse length, a resonant pulse has $\lambda_l/\lambda_p = 0.5$, where in contrast at the critical density, a 100 fs pulse has $\lambda_l/\lambda_p \approx 30$. An attractive alternative is provided by the phenomenon of self-modulation[5,27–30], where a large laser pulse ($\lambda_l/\lambda_p \gg 1$) becomes spontaneously broken into units of length λ_p and reproduces the desired wakefield behavior. This regime is called self-modulated LWFA or SM-LWFA, and is likely

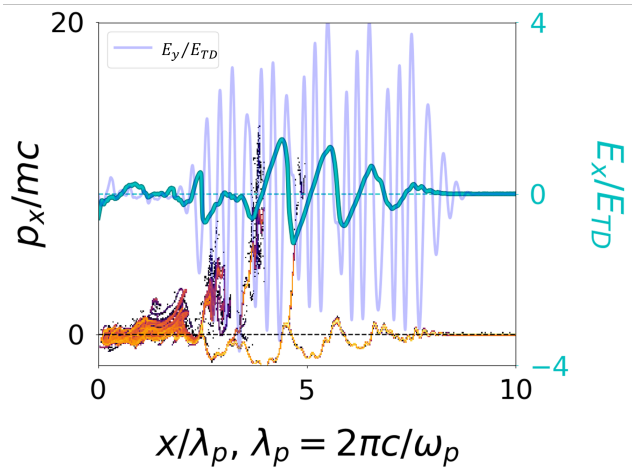

Fig. 4. A demonstration of the self-modulation of a laser pulse into resonant pieces in the "blue" regime of $n_c/n_e = 10$. Here $\lambda_{lp}/\lambda_p = 5$. The time step is $t = 9.2\tau_p$. (Similar run in Nicks *et al.*, 2019[19]).

much more amenable to fibers than the resonant pulse case. Stated simply, fibers generally prefer a longer, low-amplitude pulse to a short, intense pulse.

To demonstrate the onset of SM-LWFA, a low-density plasma of $n_c/n_e = 10$ and $a_0 = 1$ is injected with laser pulse with length ($\lambda_l/\lambda_p = 5$), as is shown in Fig. 4.[19] As progressive peaks pass a point in the plasma, the wakefield is strengthened, and ultimately the strength of the wakefield is enhanced in the self-modulated cases compared to that of the resonant case. Electron acceleration is also seen following the wakefield.

Applying this technique to a fiber laser case, Fig. 5a shows the case of 15 coherently added fiber lasers at $a_0 = 0.01$ with $n_c/n_e = 10$. The pulse is now Gaussian, also for practical considerations, with FWHM a pulse length of 100 fs. For self-modulation, it is desirable that the laser power be greater than the critical power,[24] while in this case, without considering laser guiding conditions, this condition may not be satisfied. (A rough calculation using a laser spot size of $\pi\lambda_p^2$ gives a laser power of 7.5 GW, while the critical power is given by $P_c = 17(n_c/n_e)$ GW = 170 GW.) Nonetheless, substantial acceleration in Fig. 5a is seen up to nearly 1 MeV.

Many low-energy electrons are accelerated as well. This coupling to bulk electrons may be caused by the generation of lower-frequency laser components through Raman forward scattering, which is expected in the presence of a long laser pulse.[31–33] A spectral analysis of the laser field in Fig. 5a reveals the presence of down-shifted frequency components at $\omega = \omega_0 - \omega_p$ and $\omega = \omega_0 - 2\omega_p$, as well as a small up-shifted component at $\omega = \omega_0 + \omega_p$, where ω_0 is the nominal laser frequency.

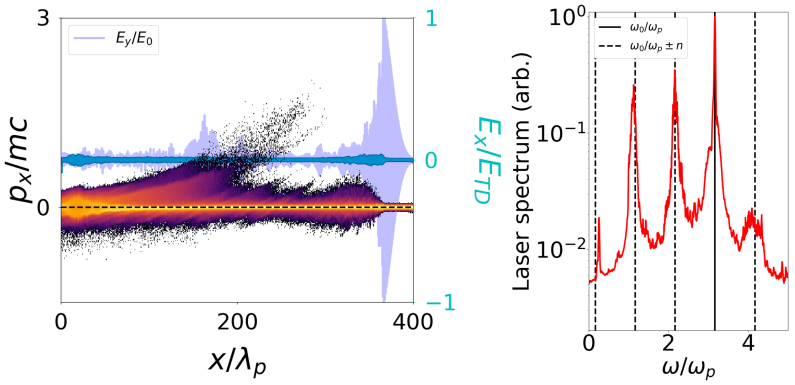

(a). Self-Modulation

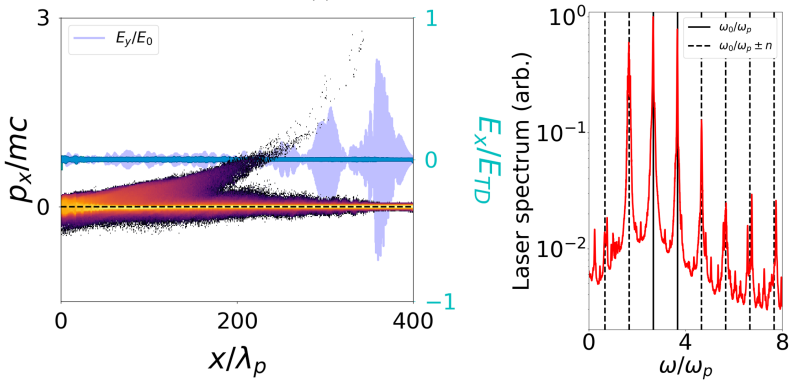

(b). Beat-Wave

Fig. 5. The electron phase space and field structure (left) for the case of a 100 fs pulse at $n_c/n_e = 10$, as well as the laser (E_y) frequency spectrum (right). Fifteen lasers each contributing intensity $a_0 = 0.01$ are coherently added, demonstrating practical parameters for fiber laser applications. In 5a, the laser pulse undergoes self-modulation, while in 5b, each of the five laser contributions is further divided into two components that beat at ω_p, thus resonantly seeding the wakefield (beat-wave acceleration). Note that here the laser field E_y is normalized with respect to the initial combined amplitude E_0 of all the fiber contributions. For the frequency spectra, solid vertical lines indicate the nominal laser frequency (ω_0/ω_p) while dashed lines indicate harmonics, which differ from the nominal frequency by some integer multiple n of the plasma frequency ω_p.

These components arise almost immediately after the laser enters, and begins interacting with, the plasma. With $n_c/n_e = 10$ in this case, $\omega_0/\omega_p = \sqrt{10} \approx 3.2$. A frequency down-shifted from this value in multiples of ω_p thus becomes very close to resonance with ω_p; the two down-shifted components $\omega = \omega_0 - \omega_p$ and $\omega = \omega_0 - 2\omega_p$ are equivalent to a laser with nominal density ratios of $n_c/n_e = 5$ and $n_c/n_e = 1.25$, respectively. The latter of these values is firmly within the "black tsunami" regime

of Figs. 1 and 3. Further down-shifting is suppressed because frequencies lower than ω_p would not be able to resonantly excite the Raman forward scattering instability and would be immediately absorbed by the plasma.

Another approach using practical fiber laser parameters is the laser beat-wave accelerator,[3,34] which was used historically in the early years of LWFA. In this scheme, two lasers with frequencies differing by ω_p create a modulation at the plasma frequency and resonantly excite the wakefield. Exploration of this possibility at $n_c/n_e = 10$ with a 100 fs Gaussian pulse and 15 $a_0 = 0.01$ lasers, each divided into two equal components separated in frequency by ω_p, shown in Fig. 5b, yielded slightly more efficient acceleration, with electrons reaching energies slightly in excess of 1 MeV. This relatively clean acceleration is expected given the seeded plasma oscillation and provides a confirmation of the physics of the pre-modulated laser field. As in the self-modulating case, here a lower laser harmonic equivalent to $n_c/n_e = 4$ is seen, as well as harmonics higher than the nominal frequency, the former perhaps aiding bulk acceleration of electrons and the latter pulling the highest-energy electrons past the energies reached in self-modulated case (Fig. 5a).

In these examples, an initially "blue" wave is converted into a "black" wave that can efficiently accelerate low-energy electrons even at very low laser intensity. Together with a variable number of coherently added fibers, this effect may provide substantial practical flexibility for a medical fiber laser application. For instance, if an optimized setup required an even lower individual laser intensity than 10^{14} W cm^{-2}, the target density could be modestly lowered, preserving the bulk flow of electrons in the desired energy range. Furthermore, if a beat-wave laser is possible, a potentially cleaner electron beam can also be produced if desired. It is remarkable that these benefits derive from the requirement of a long laser pulse, which can be considered one of the "limitations" of fiber lasers.

4. Electron Tissue Penetration

We may now consider more closely the interaction of an electron population like those in Figs. 3 and 5 with human tissue for radiation therapy. Conventional radiation therapy typically relies on exposing the body to an external source of radiation, whether X-ray, gamma-ray, protons, or electrons. In this process, the radiation passes through a significant depth of healthy tissue, causing collateral cellular damage. Three techniques to avoid this collateral damage include intraoperative radiation therapy (IORT),[10] where the source of radiation is surgically brought to the tumor, brachytherapy, in which the laser is injected into the body, or endoscopic radiation therapy (ESRT), where a small endoscope is internally brought to the tumor site. Consequently, in all of these cases, the radiation produced need only penetrate a short distance, perhaps millimeters or less. In such a scheme, the distribution in Figs. 3 and 5, possessing a large spread of low-energy electrons, may be particularly fitting. The recent development of coherent networks of fiber lasers (CAN)[14] has allowed LWFA to branch into this new and distinct application.

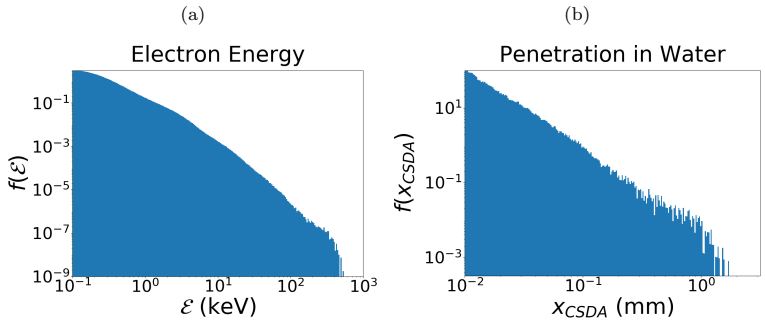

Fig. 6. Electron penetration in the high-density LWFA regime. (6a) shows the normalized electron energy distribution for setup in figure 5a, which models a bundle of 15 fiber lasers each with $a_0 = 0.01$ coherently added with plasma density $n_c/n_e = 10$ and a pulse length of 100 fs. (6b) shows the resulting normalized distribution of electron penetration depth in the continuous slowing-down approximation (CSDA).

The penetration depth in human tissue can be approximated by integrating the stopping power of electrons in water, giving the stopping distance in the continuous slowing-down approximation (CSDA).[35,36] At the critical density, the distribution of low-energy electrons in Fig. 5a has the energy distribution shown in Fig. 6a. This distribution $f(\mathcal{E})$ corresponds to a maximum penetration depth x_{CSDA} in water of about $\lesssim 1$ mm, as is shown in Fig. 6b as a function of x_{CSDA}. Tuning the plasma density allows control of the penetration depth. By changing the density of the irradiated material, the penetration depth can be tuned to the desired value; lower material density will give deeper penetration. The laser intensity a_0 or number of fibers can also be tuned for the desired electron energies produced. As an additional benefit, near the critical density, a significant acceleration of the bulk population of electrons occurs, potentially creating a far larger overall dose of radiation than would occur for more typical wakefield acceleration. This combination of a large dose and shallow, yet tunable, penetration may be ideal for intraoperative, brachytheraputic, and endoscopic medical applications.

5. Conclusions

We have studied the dynamics of LWFA in the high-density regime. In this domain, where $n_c/n_e \sim O(1)$, sheath dynamics emerges with an important role, producing a large flux of low-energy electrons (the "black tsunami" regime). Furthermore, we have found that the self-modulation or Raman forward-scattering process allows a conversion of the "blue" or "grey" regimes into the "black" regime, providing efficient generation of a bulk flow of low-energy electrons despite the presence of a density ratio n_c/n_e greater than unity. Along with the invention of the Coherent Amplification Network (CAN)[14] fiber laser technology, these dynamical character-

istics in the appropriately chosen regime of operation open a pathway to creating far more compact electron radiation sources through LWFA and thereby a radically new radiotherapy using compact electron sources.

Regarding the material to be irradiated by the laser, nanomaterials with an open structure, such as carbon nanotubes[15] or porous alumina, present an attractive means for achieving the critical density of a 1-micron laser (approximately 10^{21} cm^{-3}) while avoiding the presence of ionized gas inside of the body. Such a medium would also provide the benefit of guiding the laser. It might also be possible to tailor the design of the nanomaterial to suit the desired plasma density.

One potential challenge of this approach is that the population of accelerated electrons generated by LWFA at high density is non-monoenergic and probably of high emittance. We may also strive to further increase the efficiency. Toward such a purpose we may wish to employ a graded density of plasma to control the phase gradation of the wakefield.[37,38] Nonetheless, interesting physics has already emerged from these efforts, and the richness of a new regime is evident. Within the last decade, the technology needed to realize endoscopic electron therapy through LWFA has come of age, and serious endeavors for implementation may now proceed.

Acknowledgments

The present paper arose from the term-project efforts of the students in the tri-campus (UCI, UCLA, UCSD) graduate physics course Special Topics in Plasma Physics PHY249, "Nonlinear Plasma Physics" (Winter, 2019), led by the instructor T. Tajima. We also tried to tie plasma physics with other disciplines such as medical physics and geophysics to broaden the students' experience in physics. The tri-campus plasma physics graduate course was launched in academic year 2018, and this course was one of three such courses. The materials are partially available on Google Drive upon request. This original work is found in B. S. Nicks, S. Hakimi, E. Barraza-Valdez, K. D. Chesnut, G. H. DeGrandchamp, K. R. Gage, D. B. Housley, G. Huxtable, G. Lawler, D. J. Lin, P. Manwani, E. C. Nelson, G. M. Player, M. W. L. Seggebruch, J. Sweeney, J. E. Tanner, K. Thompson, and T. Tajima, Electron Dynamics in the High-Density Laser-Wakefield Acceleration Regime, Submitted to Phys. Rev. Accel. Beams (2019)[19]. We are thankful for discussions with J. Wheeler, J. C. Chanteloup, X. Yan, and N. Beier. This work was partially supported by the Norman Rostoker Fund at UCI.

References

1. F. M. Khan, *The Physics of Radiation* (Lippincott Williams & Wilkins, Philadelphia, PA, 2010).
2. T. Tajima, K. Nakajima and G. Mourou, Laser acceleration, *La Rivista del Nuovo Cimento* **40**, 33 (Jan 2017).
3. T. Tajima and J. M. Dawson, Laser electron accelerator, *Phys. Rev. Lett.* **43**, 267 (Jul 1979).

4. K. Nakajima *et al.*, Laser wakefield accelerator experiments using 1 ps 30 TW Nd:glass laser, in *Proceedings of International Conference on Particle Accelerators*, (Washington, DC, 1993).
5. K. Nakajima *et al.*, A proof-of-principle experiment of laser wakefield acceleration, *Phys. Scr.* **T52**, 61 (Jan 1994).
6. D. Strickland and G. Mourou, Compression of amplified chirped optical pulses, *Opt. Commun.* **56**, p. 219 (1985).
7. T. Tajima, Prospect for compact medical laser accelerators, *J. Jpn. Soc. Therp. Radiat. Oncol.* **9**, 83 (1997).
8. C. Chiu, M. Fomytskyi, F. Grigsby, F. Raischel, M. C. Downer and T. Tajima, Laser electron accelerators for radiation medicine: A feasibility study, *Med. Phys.* **31**, 2042 (2004).
9. K. K. Kainz, K. R. Hogstrom, J. A. Antolak, P. R. Almond, C. D. Bloch, C. Chiu, M. Fomytskyi, F. Raischel, M. Downer and T. Tajima, Dose properties of a laser accelerated electron beam and prospects for clinical application, *Med. Phys.* **31**, 2053 (2004).
10. A. Giulietti, N. Bourgeois, T. Ceccotti, X. Davoine, S. Dobosz, P. D'Oliveira, M. Galimberti, J. Galy, A. Gamucci *et al.*, Intense γ-ray source in the giant-dipole-resonance range driven by 10-TW laser pulses, *Phys. Rev. Lett.* **101**, p. 105002 (Sep 2008).
11. A. Giulietti (ed.), *Laser-Driven Particle Acceleration Towards Radiobiology and Medicine* (Springer International Publishing, Switzerland, 2016).
12. K. Nakajima, J. Yuan, L. Chen and Z. Sheng, Laser-driven very high energy electron/photon beam radiation therapy in conjunction with a robotic system, *Applied Sciences* **5**, 1 (3 2015).
13. K. Nakajima, Laser-driven electron beam and radiation sources for basic, medical and industrial sciences, *Proceedings of the Japan Academy, Series B* **91**, 223 (2015).
14. G. Mourou, W. Brocklesby, T. Tajima and J. Limpert, The future is fibre accelerators, *Nat. Photonics* **7**, p. 258 (2013).
15. T. Tajima, Laser acceleration in novel media, *Eur. Phys. J. Spec. Top.* **223**, 1037 (May 2014).
16. N. V. Myung, J. Lim, J.-P. Fleurial, M. Yun, W. West and D. Choi, Alumina nanotemplate fabrication on silicon substrate, *Nanotech.* **15**, 833 (apr 2004).
17. X. Zhang, T. Tajima, D. Farinella, Y. Shin, G. Mourou, J. Wheeler, P. Taborek, P. Chen, F. Dollar and B. Shen, Particle-in-cell simulation of x-ray wakefield acceleration and betatron radiation in nanotubes, *Phys. Rev. Accel. Beams* **19**, p. 101004 (Oct 2016).
18. F. Sylla, A. Flacco, S. Kahaly, M. Veltcheva, A. Lifschitz, V. Malka, E. d'Humières, I. Andriyash and V. Tikhonchuk, Short intense laser pulse collapse in near-critical plasma, *Phys. Rev. Lett.* **110**, p. 085001 (Feb 2013).
19. B. S. Nicks *et al.*, Electron dynamics in the high-density laser-wakefield acceleration regime, *Phys. Rev. Accel. Beams (Submitted)* .
20. F. Mako and T. Tajima, Collective ion acceleration by a reflexing electron beam: Model and scaling, *The Physics of Fluids* **27**, 1815 (1984).
21. B. Rau, T. Tajima and H. Hojo, Coherent electron acceleration by subcycle laser pulses, *Phys. Rev. Lett.* **78**, 3310 (Apr 1997).
22. M. T. Hassan *et al.*, Optical attosecond pulses and tracking the nonlinear response of bound electrons, *Nature (London)* **530**, p. 66 (2016).
23. H. Lamb, in *Hydrodynamics*, (Dover Publications, New York, 1945), New York, ch. 8.
24. E. Esarey, C. B. Schroeder and W. P. Leemans, Physics of laser-driven plasma-based electron accelerators, *Rev. Mod. Phys.* **81**, 1229 (Aug 2009).

25. E. Fourkal, B. Shahine, M. Ding, J. S. Li, T. Tajima and C.-M. Ma, Particle in cell simulation of laser-accelerated proton beams for radiation therapy, *Med. Phys.* **29**, 2788 (2002).
26. G. P. Agrawal, *Nonlinear Fiber Optics* (Oxford:Academic, 2013).
27. N. E. Andreev, L. M. Gorbunov, A. A. Pogasova, R. R. Ramazashvili and V. I. Kirsanov, Resonant excitation of wake fields by a laser pulse in a plasma, *JETP Lett.* **55**, 571 (1992), [Pisma Zh. Eksp. Teor. Fiz.55,551(1992)].
28. J. Krall, A. Ting, E. Esarey and P. Sprangle, Self-modulated laser wake field acceleration, in *Proceedings of the 1993 Particle Accelerator Conference*, (Washington, DC, 1993).
29. K. Nakajima *et al.*, Observation of ultrahigh gradient electron acceleration by a self-modulated intense short laser pulse, *Phys. Rev. Lett.* **74**, 4428 (May 1995).
30. A. Modena *et al.*, Electron acceleration from the breaking of relativistic plasma waves, *Nature (London)* **377**, 606 (1995).
31. C. Joshi, T. Tajima, J. M. Dawson, H. A. Baldis and N. A. Ebrahim, Forward raman instability and electron acceleration, *Phys. Rev. Lett.* **47**, 1285 (Nov 1981).
32. D. L. Fisher and T. Tajima, Enhanced raman forward scattering, *Phys. Rev. E* **53**, 1844 (Feb 1996).
33. W. B. Mori, The physics of the nonlinear optics of plasmas at relativistic intensities for short-pulse lasers, *IEEE Journal of Quantum Electronics* **33**, 1942 (Nov 1997).
34. M. N. Rosenbluth and C. S. Liu, Excitation of plasma waves by two laser beams, *Phys. Rev. Lett.* **29**, 701 (Sep 1972).
35. M. J. Berger, J. S. Coursey and M. A. Zucker, ESTAR, PSTAR, and ASTAR: Computer programs for calculating stopping-power and range tables for electrons, protons, and helium ions (version 1.21) (Jan 1999).
36. D. K. Brice, Stopping powers for electrons and positrons (ICRU report 37; international commission on radiation units and measurements, Bethesda, Maryland, USA, 1984), *Nuclear Instruments and Methods in Physics Research Section B: Beam Interactions with Materials and Atoms* **12**, 187 (1985).
37. R. Hu, H. Lu, Y. Shou, C. Lin, H. Zhuo, C. Chen and X. Yan, Brilliant GeV electron beam with narrow energy spread generated by a laser plasma accelerator, *Phys. Rev. Accel. Beams* **19**, p. 091301 (Sep 2016).
38. A. Döpp, C. Thaury, E. Guillaume, F. Massimo, A. Lifschitz, I. Andriyash, J.-P. Goddet, A. Tazfi, K. Ta Phuoc and V. Malka, Energy-chirp compensation in a laser wakefield accelerator, *Phys. Rev. Lett.* **121**, p. 074802 (Aug 2018).